 CMC, vol.5, no.1, pp.43-61, 2007

A New Locking Free Higher Order Finite Element Formulation for Composite Beams.

M.V.V.S. Murthy[1], S. Gopalakrishnan[2,3] and P.S. Nair[4]

Abstract: A refined 2-node, 7 DOF/node beam element formulation is presented in this paper. This formulation is based on higher order shear deformation theory with lateral contraction for axial-flexural-shear coupled deformation in asymmetrically stacked laminated composite beams. In addition to axial, transverse and rotational degrees of freedom, the formulation also incorporates the lateral contraction and its higher order counterparts as degrees of freedom. The element shape functions are derived by solving the static part of the governing equations. The element considers general ply stacking and the numerical results shows that the element exhibits super convergent property. The efficiency of the element in capturing both the static and dynamic inter-laminar stresses is demonstrated. The accuracy of the element to capture free vibration and wave propogation responses with small problem sizes is also demonstrated.

Keyword: Laminated composite, Higher order theory, Shear deformation, lateral contraction, Asymmetric ply stacking, Wave propogation, High frequency.

1 Introduction

Fiber reinforced laminated composite constructions are in extensive use in many structural applications in aerospace, automotive and civil engineering industry. The nature of laminated construction gives rise to higher ratio of extensional moduli to shear moduli. Composites usually fail due to delamination mode of failure. This is caused due to interlaminar stresses (both normal and shear) developed in the composite. The presence of axial-bending coupling in composites accelerates the process of delamination formation. Also minute discontinuties can cause the delamintation in composite. Prediction of interlaminar stresses in beams (τ_{xz} and σ_{zz}) is one of the challenging tasks in the analysis of composites. There are three well known beam theories available for analysis, namely the Euler-Bernoulli Theory (EBT), the Timoshenko beam theory also known as First order Shear deformation Theory (FSDT) and the Higher order Shear Deformation Theory (HSDT). In the EBT, the displacement field is such that it gives both τ_{xz} and σ_{zz} equal to zero. In FSDT, although τ_{xz} is not equal to zero, the solution always yields constant interlaminar stress, which is not the true state. HSDT, although gives better prediction of interlaminar stresses compared to FSDT, it still does not consider the lateral contraction effects due to Poisson's ratio, which is one of the important parameter in contributing to the interlaminar stresses.

Alternately, the layer-wise concept can be considered to determine the interlaminar stresses accurately. Here the main disadvantage is that the degrees of freedom involved is directly dependent on the number of layers and hence as the layers grow, the cost of computation also proportionally increases. Pioneering works in this aspect can be found in Kim and Atluri (1994) and Reddy (1997).

To further understand the need for higher order finite element(FE) formulation, the three existing theories are reviewed here. EBT theory is suited

[1] ISRO Satellite Center (ISAC), Vimanapura Post, Bangalore 560017, India

[2] Department of Aerospace Engineering, Indian Institute of Science, Bangalore 560012, India

[3] Corresponding Author e-mail: krishnan@aero.iisc.ernet.in, Tel: 91-080-22933019, Fax: 91-080-23600134

[4] ISRO Satellite Center (ISAC), Vimanapura Post, Bangalore 560017, India

for only long thin beams, where shear deformation is not significant. Since the slopes are derived from transverse displacements, the FE formulation, it requires C^1 continuity. FSDT on the other hand requires computation of shear correction factors, which are in many cases quite cumbersome. Generally the method employed for the computation of shear correction factor is by equilibrating the calculated strain energy to the actual strain energy as shown in Kouri and Atluri (1993). Whitney (1973) derived the shear correction factors for composite with general ply-stacking for static analysis, while for dynamic analysis Doyle (1997) & Mahapatra and Gopalakrishnan (2003) have derived the same for isotropic and composite waveguides respectively. Introduction of shear deformation destroys the assumption of plane sections remaining plane after bending and hence in FSDT, the slope is interpolated independently and not derived from transverse displacement. Hence, C^0 continuity is sufficient for FE formulation. However, when FSDT element is used for thin beam cases, the element will give responses that are many order smaller than the correct response. This problem is called the shear locking problem and FSDT finite elements require special treatment to alleviate this problem. HSDT proposed by Heyliger and Reddy (1988) do not require shear correction factor as it approximates the shear stresses across the beam depth accurately. Again, this theory interpolates the slopes independent of transverse displacement. However, higher order degrees of freedom are required to be introduced to take care of improved interlaminar stress predictions. As before, this element will lock if proper care is not taken. The effect of locking (both shear locking and the thickness locking) has been extensively dealt by Li, Soric, Jarak, and Atluri (2005) based on the meshless local Petro-Galerkin formualtion. The simplest explanation of locking and the various means to elminate it are discussed by Atluri (2005).

All the theories (EBT, FSDT and HSDT), however do not take into account, the effect of lateral contraction, which contributes to the transverse normal stress(σ_{zz}). This stress is required to model the peeling effect of the laminate. There are several HSDT reported in the literature. In the above paragraphs, we have discussed only the HSDT proposed by Heyliger and Reddy (1988). This is because we have used the results from the above theory for comparison of results obtained by the formulation presented in this paper. However, HSDT proposed by Lo, Christensen, and Wu (1977a,b) considers the effect of lateral contraction. Vinayak, Prathap, and Naganarayana (1996a,b) have formulated beam elements based on the above theory using field consistent approach.

As mentioned before, one of the major problems encountered by C^0 beam elements is the shear locking problem when used for thin beams. This problem is well researched and there are many papers reported in the archival literature. Methods like assumed strain field and reduced integration has been used in the past. A locking free hybrid assumed-strain, plate element is derived within the framework of the FSDT and is presented by Cazzani, Garusi, Tralli, and Atluri (2005). Here the stresses are derived by integrating the equilibrium equations in each lamina. Similarly, Koiter's asymptotic method is combined with the assumed strain solid shell element formulation for post-buckling analysis of sandwich structures which has been presented by JihanKim, YongHyupKim, and Lee (2004) and is shown that this element is free of locking behaviour. Other methods like *choosing* an appropriate polynomial for the field variables, *a priori*, locking can be eliminated. The approach employed here is that instead of choosing an arbitrary polynomial for the field variable we derive this by solving the static part of the governing differential equations. The solutions thereby, is then used as interpolating function for element formulation. As the derived polynomial satisfies the govering differential equations, locking is automatically eliminated. In addition, many constants in the interpolating functions of the field variables becomes functions of material and sectional properties of the beam. In this paper, we present this novel approach to formulate a higher order 2-node composite beam element that has 7 degrees of freedom per node, out of which 4 are

higher order degrees of freedom, which also includes the lateral contraction, while other three represent the usual axial, transverse and rotation degrees of freedom. The major difference is that the equilibrium is satisfied by assuming suitable displacement field for the four higher order degrees of freedom and equilibrium equations corresponding to axial,transverse and rotation degrees of freedom are solved *exactly*.

The paper is organized as follows. First the governing equations for higher order composite beam is derived and this is followed by the finite element formulation and then a detailed section on Numerical results are presented where the element is tested for various problems in statics, free vibration and wave propogation problems. The results from the formulated element are compared with 2D FEM and also with results available in literature. Wave solutions are compared with 2D FE solution.

2 Governing Differential Equations

Considering the HSDT as reported by Lo, Christensen, and Wu (1977a), the axial and transverse displacement fields are expressed as, $\{\overline{d}\} = \{U(x,y,z,t), W(x,y,z,t)\}^T$

$$U(x,y,z,t) = u_0(x,t) + z\theta(x,t) + z^2\overline{\theta}(x,t) + z^3\overline{\overline{\theta}}(x,t)\,, \tag{1a}$$

$$W(x,y,z,t) = w_0(x,t) + z\psi(x,t) + z^2\overline{\psi}(x,t)\,, \tag{1b}$$

where U and W are the displacements in X and Z directions at any material point in the (X,Z) plane. u and w are the longitudinal and transverse displacements along the the beam reference plane (X,Y). θ is the rotation of the normal to the cross-section about Y-axis z is the depth of the material point measured from the beam reference plane along positive Z-axis. $\overline{\theta}$, $\overline{\overline{\theta}}$ represents the warping effect and ψ and $\overline{\psi}$ represents the contraction/expansion effect as shown in Fig. 1.

The strains can be written as,

$$\varepsilon_{xx} = \frac{\partial u}{\partial x} + z\frac{\partial \theta}{\partial x} + z^2\frac{\partial \overline{\theta}}{\partial x} + z^3\frac{\partial \overline{\overline{\theta}}}{\partial x} \tag{2a}$$

$$\varepsilon_{zz} = \psi + 2z\overline{\psi} \tag{2b}$$

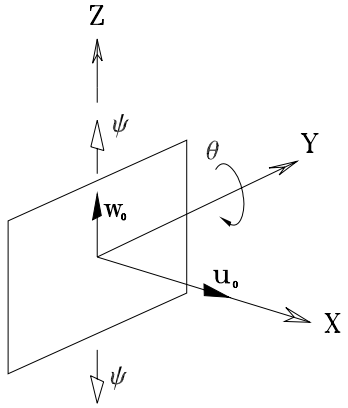

Figure 1: Beam cross-section in $Y-Z$ plane.

$$\gamma_{xz} = \theta + \frac{\partial w}{\partial x} + z(2\overline{\theta} + \frac{\partial \psi}{\partial x}) + z^2(3\overline{\overline{\theta}} + \frac{\partial \overline{\psi}}{\partial x})\,. \tag{2c}$$

The constitutive relation is derived from the constitutive law assuming plane stress condition in the $X-Z$ plane, The constitutive relation for a general orthotropic laminate is given by,

$$\begin{Bmatrix} \sigma_{xx} \\ \sigma_{yy} \\ \sigma_{zz} \\ \tau_{yz} \\ \tau_{xz} \\ \tau_{xy} \end{Bmatrix} = \begin{bmatrix} \overline{Q}_{11} & \overline{Q}_{12} & \overline{Q}_{13} & 0 & 0 & \overline{Q}_{16} \\ \overline{Q}_{21} & \overline{Q}_{22} & \overline{Q}_{23} & 0 & 0 & \overline{Q}_{26} \\ \overline{Q}_{31} & \overline{Q}_{32} & \overline{Q}_{33} & 0 & 0 & \overline{Q}_{36} \\ 0 & 0 & 0 & \overline{Q}_{44} & \overline{Q}_{45} & 0 \\ 0 & 0 & 0 & \overline{Q}_{45} & \overline{Q}_{55} & 0 \\ \overline{Q}_{16} & \overline{Q}_{26} & \overline{Q}_{36} & 0 & 0 & \overline{Q}_{66} \end{bmatrix} \begin{Bmatrix} \varepsilon_{xx} \\ \varepsilon_{yy} \\ \varepsilon_{zz} \\ \gamma_{yz} \\ \gamma_{xz} \\ \gamma_{xy} \end{Bmatrix}, \tag{3}$$

The expressions for $\overline{Q}_{ij}$, transformed elasticity matrix from material coordinate to the laminate coordinate in the $X-Z$ plane can be found in standard texts (e.g. Reddy (1997)) and is given as,
$\overline{Q}_{11} = Q_{11}\,c^4 - 4\,Q_{16}\,c^3\,s + 2\,(Q_{12} + 2\,Q_{66})\,c^2\,s^2 - 4\,Q_{26}\,c\,s^3 + Q_{22}\,s^4$
$\overline{Q}_{12} = Q_{12}\,c^4 + 2\,(Q_{16} - Q_{26})\,c^3\,s + (Q_{11} + Q_{22} - 4\,Q_{66})\,c^2\,s^2 +$
$2\,(Q_{26} - Q_{16})\,c\,s^3 + Q_{12}\,s^4$
$\overline{Q}_{13} = Q_{13}\,c^2 - 2\,Q_{36}\,c\,s + Q_{23}\,s^2$

$\overline{Q}_{16} = Q_{16}\ c^4 + (Q_{11} - Q_{12} - 2\ Q_{66})\ c^3\ s + 3\ (Q_{26} - Q_{16})\ c^2\ s^2 + (2\ Q_{66} + Q_{12} - Q_{22})\ c\ s^3 - Q_{26}\ s^4$
$\overline{Q}_{22} = Q_{22}\ c^4 + 4\ Q_{26}\ c^3\ s + 2\ (Q_{12} + 2\ Q_{66})\ c^2\ s^2 + 4\ Q_{16}\ c\ s^3 + Q_{11}\ s^4$
$\overline{Q}_{23} = Q_{23}\ c^2 + 2\ Q_{36}\ c\ s + Q_{13}\ s^2$
$\overline{Q}_{26} = Q_{26}\ c^4 + (Q_{12} - Q_{22} + 2\ Q_{66})\ c^3\ s + 3\ (Q_{16} - Q_{26})\ c^2\ s^2 + (Q_{11} - Q_{12} - 2\ Q_{66})\ c\ s^3 - Q_{16}\ s^4$
$\overline{Q}_{33} = Q_{33}$
$\overline{Q}_{36} = (Q_{13} - Q_{23})\ c\ s + Q_{36}\ (c^2 - s^2)$
$\overline{Q}_{44} = Q_{44}\ c^2 + Q_{55}\ s^2 + 2\ Q_{45}\ c\ s$
$\overline{Q}_{45} = Q_{45}\ (c^2 - s^2) + (Q_{55} - Q_{44})\ c\ s$
$\overline{Q}_{55} = Q_{55}\ c^2 + Q_{44}\ s^2 - 2\ Q_{45}\ c\ s$
$\overline{Q}_{66} = 2\ (Q_{16} - Q_{26})\ c^3\ s + (Q_{11} + Q_{22} - 2\ Q_{12} - 2\ Q_{66})\ c^2\ s^2 + 2\ (Q_{26} - Q_{16})\ c\ s^3 + Q_{66}\ (c^4 + s^4)$

where c = cos(θ) and s = sin(θ).

Assuming that the beam deforms in the $X - Z$ plane, we have σ_{yy}, τ_{yz} and τ_{xy} are zero. From Eq. 3 we have,

$$\sigma_{yy} = 0 \rightarrow \quad \left[\overline{Q}_{11}\ \overline{Q}_{22}\ \overline{Q}_{23}\ \overline{Q}_{26}\right] \left\{ \begin{array}{c} \varepsilon_{xx} \\ \varepsilon_{yy} \\ \varepsilon_{zz} \\ \gamma_{xy} \end{array} \right\} = 0 \tag{4a}$$

$$\tau_{yz} = 0 \rightarrow \quad \left[\overline{Q}_{44}\ \overline{Q}_{45}\right] \left\{ \begin{array}{c} \gamma_{yz} \\ \gamma_{xz} \end{array} \right\} = 0 \tag{4b}$$

$$\tau_{xy} = 0 \rightarrow \quad \left[\overline{Q}_{16}\ \overline{Q}_{26}\ \overline{Q}_{36}\ \overline{Q}_{66}\right] \left\{ \begin{array}{c} \varepsilon_{xx} \\ \varepsilon_{yy} \\ \varepsilon_{zz} \\ \gamma_{xy} \end{array} \right\} = 0 \tag{4c}$$

Equations 4a-4c and Eq. 3 yield,

$$\varepsilon_{yy} = \frac{(\overline{Q}_{16}\overline{Q}_{26} - \overline{Q}_{12}\overline{Q}_{66})}{(\overline{Q}_{22}\overline{Q}_{66} - \overline{Q}_{26}^2)}\varepsilon_{xx} + \frac{(\overline{Q}_{26}\overline{Q}_{36} - \overline{Q}_{23}\overline{Q}_{66})}{(\overline{Q}_{22}\overline{Q}_{66} - \overline{Q}_{26}^2)}\varepsilon_{zz} \tag{5a}$$

$$\gamma_{yz} = \frac{\overline{Q}_{45}}{\overline{Q}_{44}}\gamma_{xz} \tag{5b}$$

$$\gamma_{xy} = \frac{(\overline{Q}_{16}\overline{Q}_{22} - \overline{Q}_{12}\overline{Q}_{26})}{(\overline{Q}_{26}^2 - \overline{Q}_{22}\overline{Q}_{66})}\varepsilon_{xx} + \frac{(\overline{Q}_{22}\overline{Q}_{36} - \overline{Q}_{23}\overline{Q}_{26})}{(\overline{Q}_{26}^2 - \overline{Q}_{22}\overline{Q}_{66})}\varepsilon_{zz} \tag{5c}$$

Subsituting equations 5a-5c into Eq. 3 we get the constitutive matrix as,

$$\left\{ \begin{array}{c} \sigma_{xx} \\ \sigma_{zz} \\ \tau_{xz} \end{array} \right\} = \left[\begin{array}{ccc} \overline{Q}_{11}^* & \overline{Q}_{13}^* & 0 \\ \overline{Q}_{13}^* & \overline{Q}_{33}^* & 0 \\ 0 & 0 & \overline{Q}_{55}^* \end{array} \right] \left\{ \begin{array}{c} \varepsilon_{xx} \\ \varepsilon_{zz} \\ \gamma_{xz} \end{array} \right\}, \tag{6}$$

where the relations for $\overline{Q}_{11}^*, \overline{Q}_{13}^*, \overline{Q}_{33}^*$ and $\overline{Q}_{55}^*$ are,

$$\overline{Q}_{11}^* = \overline{Q}_{11} + \overline{Q}_{12}\left[\frac{(\overline{Q}_{16}\overline{Q}_{22} - \overline{Q}_{12}\overline{Q}_{26})}{(\overline{Q}_{26}^2 - \overline{Q}_{22}\overline{Q}_{66})}\right] + \overline{Q}_{16}\left[\frac{(\overline{Q}_{16}\overline{Q}_{22} - \overline{Q}_{12}\overline{Q}_{26})}{(\overline{Q}_{26}^2 - \overline{Q}_{22}\overline{Q}_{66})}\right] \tag{7a}$$

$$\overline{Q}_{13}^* = \overline{Q}_{13} + \overline{Q}_{12}\left[\frac{(\overline{Q}_{36}\overline{Q}_{26} - \overline{Q}_{23}\overline{Q}_{66})}{(\overline{Q}_{22}\overline{Q}_{66} - \overline{Q}_{26}^2)}\right] + \overline{Q}_{16}\left[\frac{(\overline{Q}_{36}\overline{Q}_{22} - \overline{Q}_{23}\overline{Q}_{26})}{(\overline{Q}_{26}^2 - \overline{Q}_{22}\overline{Q}_{66})}\right] \tag{7b}$$

$$\overline{Q}_{33}^* = \overline{Q}_{33} + \overline{Q}_{23}\left[\frac{(\overline{Q}_{36}\overline{Q}_{26} - \overline{Q}_{23}\overline{Q}_{66})}{(\overline{Q}_{22}\overline{Q}_{66} - \overline{Q}_{26}^2)}\right] + \overline{Q}_{16}\left[\frac{(\overline{Q}_{36}\overline{Q}_{22} - \overline{Q}_{23}\overline{Q}_{26})}{(\overline{Q}_{26}^2 - \overline{Q}_{22}\overline{Q}_{66})}\right] \tag{7c}$$

$$\overline{Q}_{55}^* = \overline{Q}_{55} - \frac{\overline{Q}_{45}^2}{\overline{Q}_{44}} \tag{7d}$$

The strain energy and kinetic energy are then expressed as

$$S = \frac{1}{2}\int\int (\sigma_{xx}\varepsilon_{xx} + \sigma_{zz}\varepsilon_{zz} + \tau_{xz}\gamma_{xz})\, dA\, dx\,,$$
$$T = \frac{1}{2}\int\int \rho(\dot{U}^2 + \dot{W}^2)\, dA\, dx\,, \tag{8}$$

where A is the area of cross-section of the beam. The Lagrangian is given by,

$$\overline{L} = (T - S)\,, \tag{9}$$

Using Hamilton's principle which is given by,

$$\delta \int_{t1}^{t2} \overline{L} dt = 0 \tag{10}$$

following seven governing differential equations are obtained corresponding to seven degrees of freedom and they can be expressed as

$$-I_0\ddot{u}-I_1\ddot{\theta}-I_2\ddot{\overline{\theta}}-I_3\ddot{\overline{\overline{\theta}}}+A_{11}\frac{\partial^2 u}{\partial x^2}+B_{11}\frac{\partial^2\theta}{\partial x^2}+D_{11}\frac{\partial^2\overline{\theta}}{\partial x^2}+F_{11}\frac{\partial^2\overline{\overline{\theta}}}{\partial x^2}+A_{13}\frac{\partial\psi}{\partial x}+2B_{13}\frac{\partial\overline{\psi}}{\partial x}=0; \tag{11a}$$

$$-I_0\ddot{w}-I_1\ddot{\psi}-I_2\ddot{\overline{\psi}}+A_{55}\frac{\partial\theta}{\partial x}+2B_{55}\frac{\partial\overline{\theta}}{\partial x}+3D_{55}\frac{\partial\overline{\overline{\theta}}}{\partial x}+B_{55}\frac{\partial^2\psi}{\partial x^2}+D_{55}\frac{\partial^2\overline{\psi}}{\partial x^2}+A_{55}\frac{\partial^2 w}{\partial x^2}=0 \tag{11b}$$

$$-I_1\ddot{u}-I_2\ddot{\theta}-I_3\ddot{\overline{\theta}}-I_4\ddot{\overline{\overline{\theta}}}+B_{11}\frac{\partial^2 u}{\partial x^2}+D_{11}\frac{\partial^2\theta}{\partial x^2}+F_{11}\frac{\partial^2\overline{\theta}}{\partial x^2}+H_{11}\frac{\partial^2\overline{\overline{\theta}}}{\partial x^2}+A_{13}\frac{\partial^2\psi}{\partial x^2}+2D_{13}\frac{\partial^2\overline{\psi}}{\partial x^2}-A_{55}\theta-2B_{55}\overline{\theta}-3D_{55}\overline{\overline{\theta}}-B_{55}\frac{\partial\psi}{\partial x}-D_{55}\frac{\partial\overline{\psi}}{\partial x}-A_{55}\frac{\partial w}{\partial x}=0 \tag{11c}$$

$$-I_1\ddot{w}-I_2\ddot{\psi}-I_3\ddot{\overline{\psi}}+A_{55}\frac{\partial\theta}{\partial x}+2D_{55}\frac{\partial\overline{\theta}}{\partial x}+3F_{55}\frac{\partial\overline{\overline{\theta}}}{\partial x}+D_{55}\frac{\partial^2\psi}{\partial x^2}+F_{55}\frac{\partial^2\overline{\psi}}{\partial x^2}+B_{55}\frac{\partial^2 w}{\partial x^2}-A_{13}\frac{\partial u}{\partial x}-B_{13}\frac{\partial\theta}{\partial x}-D_{13}\frac{\partial\overline{\theta}}{\partial x}-F_{13}\frac{\partial\overline{\overline{\theta}}}{\partial x}-A_{33}\psi-2B_{33}\overline{\psi}=0 \tag{11d}$$

$$-I_2\ddot{u}-I_3\ddot{\theta}-I_4\ddot{\overline{\theta}}-I_5\ddot{\overline{\overline{\theta}}}D_{11}\frac{\partial^2 u}{\partial x^2}+F_{11}\frac{\partial^2\theta}{\partial x^2}+H_{11}\frac{\partial^2\overline{\theta}}{\partial x^2}+J_{11}\frac{\partial^2\overline{\overline{\theta}}}{\partial x^2}+D_{13}\frac{\partial\psi}{\partial x}+2F_{13}\frac{\partial\overline{\psi}}{\partial x}-2B_{55}\theta-4D_{55}\overline{\theta}-6F_{55}\overline{\overline{\theta}}-2D_{55}\frac{\partial\psi}{\partial x}-2F_{55}\frac{\partial\overline{\psi}}{\partial x}-2B_{55}\frac{\partial w}{\partial x}=0 \tag{11e}$$

$$-I_3\ddot{u}-I_4\ddot{\theta}-I_5\ddot{\overline{\theta}}-I_6\ddot{\overline{\overline{\theta}}}F_{11}\frac{\partial^2 u}{\partial x^2}+H_{11}\frac{\partial^2\theta}{\partial x^2}+J_{11}\frac{\partial^2\overline{\theta}}{\partial x^2}+L_{11}\frac{\partial^2\overline{\overline{\theta}}}{\partial x^2}+F_{13}\frac{\partial\psi}{\partial x}+2H_{13}\frac{\partial\overline{\psi}}{\partial x}-3D_{55}\theta-6F_{55}\overline{\theta}-9H_{55}\overline{\overline{\theta}}-3F_{55}\frac{\partial\psi}{\partial x}-3H_{55}\frac{\partial\overline{\psi}}{\partial x}-3D_{55}\frac{\partial w}{\partial x}=0 \tag{11f}$$

$$-I_2\ddot{w}-I_3\ddot{\psi}-I_4\ddot{\overline{\psi}}D_{55}\frac{\partial\theta}{\partial x}+2F_{55}\frac{\partial\overline{\theta}}{\partial x}+3H_{55}\frac{\partial\overline{\overline{\theta}}}{\partial x}+F_{55}\frac{\partial^2\psi}{\partial x^2}+H_{55}\frac{\partial^2\overline{\psi}}{\partial x^2}+D_{55}\frac{\partial^2 w}{\partial x^2}-2B_{13}\frac{\partial u}{\partial x}-2D_{13}\frac{\partial\theta}{\partial x}-2F_{13}\frac{\partial\overline{\theta}}{\partial x}-2H_{13}\frac{\partial\overline{\overline{\theta}}}{\partial x}-2B_{33}\psi-4D_{33}\overline{\psi}=0 \tag{11g}$$

where $\dot{(\,)}$ indicates temporal derivative. The cross-sectional stiffness coefficients associated with the above equations are

$$[A_{ij}\,B_{ij}\,D_{ij}\,F_{ij}\,H_{ij}\,J_{ij}\,L_{ij}]=b\int_{-h/2}^{+h/2}\overline{Q}_{ij}\left[1\,z\,z^2\,z^3\,z^4\,z^5\,z^6\right]dz\,, \tag{12}$$

and similarly the cross-sectional inertial coefficients are

$$I_i=b\int_{-h/2}^{+h/2}\rho z^i dz\,,\quad i=0,\cdots,6\,. \tag{13}$$

and the Force Boundary equations at the two ends $(x=0,L)$ of the beam are, prescribed as

$u_0=u_{0(\text{prescribed})}$ or

$$\left[\begin{array}{c}A_{11}\frac{\partial u}{\partial x}+B_{11}\frac{\partial\theta}{\partial x}+D_{11}\frac{\partial\overline{\theta}}{\partial x}\\+F_{11}\frac{\partial\overline{\overline{\theta}}}{\partial x}+A_{13}\psi+2B_{13}\overline{\psi}\end{array}\right]_{(\text{prescribed})}, \tag{14a}$$

$w_0=w_{0(\text{prescribed})}$ or

$$\left[\begin{array}{c}A_{55}\theta+2B_{55}\overline{\theta}+3D_{55}\overline{\overline{\theta}}\\+B_{55}\frac{\partial\psi}{\partial x}+D_{55}\frac{\partial\overline{\psi}}{\partial x}+A_{55}\frac{\partial w}{\partial x}\end{array}\right]_{(\text{prescribed})}, \tag{14b}$$

$\theta=\theta_{(\text{prescribed})}$ or

$$\left[\begin{array}{c}B_{11}\frac{\partial u}{\partial x}+D_{11}\frac{\partial\theta}{\partial x}+F_{11}\frac{\partial\overline{\theta}}{\partial x}\\+H_{11}\frac{\partial\overline{\overline{\theta}}}{\partial x}+B_{13}\psi+2D_{13}\overline{\psi}\end{array}\right]_{(\text{prescribed})}, \tag{14c}$$

$\psi=\psi_{(\text{prescribed})}$ or

$$\left[\begin{array}{c}B_{55}\theta+2D_{55}\overline{\theta}+3F_{55}\overline{\overline{\theta}}\\+D_{55}\frac{\partial\psi}{\partial x}+F_{55}\frac{\partial\overline{\psi}}{\partial x}+B_{55}\frac{\partial w}{\partial x}\end{array}\right]_{(\text{prescribed})}, \tag{14d}$$

$\overline{\theta}=\overline{\theta}_{(\text{prescribed})}$ or

$$\left[\begin{array}{c}D_{11}\frac{\partial u}{\partial x}+F_{11}\frac{\partial\theta}{\partial x}+H_{11}\frac{\partial\overline{\theta}}{\partial x}\\+J_{11}\frac{\partial\overline{\overline{\theta}}}{\partial x}+D_{13}\psi+2F_{13}\overline{\psi}\end{array}\right]_{(\text{prescribed})}, \tag{14e}$$

$\overline{\overline{\theta}}=\overline{\overline{\theta}}_{(\text{prescribed})}$ or

$$\left[\begin{array}{c} F_{11}\frac{\partial u}{\partial x}+H_{11}\frac{\partial \theta}{\partial x}+J_{11}\frac{\partial \overline{\theta}}{\partial x} \\ +L_{11}\frac{\partial \overline{\overline{\theta}}}{\partial x}+F_{13}\psi+2H_{13}\overline{\psi} \end{array}\right]_{\text{(prescribed)}}, \quad (14f)$$

$$\overline{\psi}=\overline{\psi}_{\text{(prescribed)}} \quad \text{or}$$

$$\left[\begin{array}{c} D_{55}\theta+2F_{55}\overline{\theta}+3H_{55}\overline{\overline{\theta}} \\ +F_{55}\frac{\partial \psi}{\partial x}+H_{55}\frac{\partial \overline{\psi}}{\partial x}+D_{55}\frac{\partial w}{\partial x} \end{array}\right]_{\text{(prescribed)}}, \quad (14g)$$

From equations (11), it is very clear that there exists a very strong inertial and stiffness coupling in the behaviour of the beam. We use the governing equations (11) and the associated force boundary conditions (14) for the element formulation.

3 Finite Element Formulation

Consider a beam of length L, thickness h and width b. Each node supports 7 degrees of freedom namely the axial degree of freedom u_0, the transverse degree of freedom w_0, slope θ, lateral contraction ψ and higher order degrees of freedom $\overline{\theta}$, $\overline{\overline{\theta}}$, and $\overline{\psi}$ respectively. It is well known that the introduction to lateral contraction will result in the exponential (hyperbolic) term being present in both the axial and transverse displacement field (Gopalakrishnan (2000), Chakraborty and Gopalakrishnan (2003)). However these hyperbolic terms contribute, very little to the overall response. Hence in the present case, we can assume a linear interpolation functions for higher order degrees of freedom; which is given by,

$$\overline{\theta}=C_1x+C_2;\ \overline{\overline{\theta}}=C_3x+C_4;\ \psi=C_5x+C_6;\ \overline{\psi}=C_7x+C_8\,. \quad (15)$$

The main objective here is to use the above assumed variation and obtain a solution for u_0, w_0 and θ, such that the equilibrium equations are satisfied. Considering only the static part of the first 3 governing equations we have them as;

$$+A_{11}\frac{\partial^2 u}{\partial x^2}+B_{11}\frac{\partial^2 \theta}{\partial x^2}+D_{11}\frac{\partial^2 \overline{\theta}}{\partial x^2} +F_{11}\frac{\partial^2 \overline{\overline{\theta}}}{\partial x^2}+A_{13}\frac{\partial \psi}{\partial x}+2B_{13}\frac{\partial \overline{\psi}}{\partial x}=0 \quad (16a)$$

$$A_{55}\frac{\partial \theta}{\partial x}+2B_{55}\frac{\partial \overline{\theta}}{\partial x}+3D_{55}\frac{\partial \overline{\overline{\theta}}}{\partial x} +B_{55}\frac{\partial^2 \psi}{\partial x^2}+D_{55}\frac{\partial^2 \overline{\psi}}{\partial x^2}+A_{55}\frac{\partial^2 w}{\partial x^2}=0 \quad (16b)$$

$$B_{11}\frac{\partial^2 u}{\partial x^2}+D_{11}\frac{\partial^2 \theta}{\partial x^2}+F_{11}\frac{\partial^2 \overline{\theta}}{\partial x^2} +H_{11}\frac{\partial^2 \overline{\overline{\theta}}}{\partial x^2}+A_{13}\frac{\partial^2 \psi}{\partial x^2}+2D_{13}\frac{\partial^2 \overline{\psi}}{\partial x^2} -A_{55}\theta-2B_{55}\overline{\theta}-3D_{55}\overline{\overline{\theta}} -B_{55}\frac{\partial \psi}{\partial x}-D_{55}\frac{\partial \overline{\psi}}{\partial x}-A_{55}\frac{\partial w}{\partial x}=0 \quad (16c)$$

Differentiating Eq. (16c), substituting Eq. (16a) for $\frac{\partial^2 u}{\partial x^2}$ and Eq. (16b) in Eq. (16c) we get,

$$\frac{\partial^3 \theta}{\partial x^3}=\frac{(A_{11}F_{11}-B_{11}D_{11})}{(B_{11}^2-A_{11}D_{11})}\frac{\partial^3 \overline{\theta}}{\partial x^3}+\frac{(A_{11}H_{11}-B_{11}F_{11})}{(B_{11}^2-A_{11}D_{11})}\frac{\partial^3 \overline{\overline{\theta}}}{\partial x^3} +\frac{(A_{11}B_{13}-B_{11}A_{13})}{(B_{11}^2-A_{11}D_{11})}\frac{\partial^2 \psi}{\partial x^2}+\frac{(2A_{11}D_{13}-2B_{11}B_{13})}{(B_{11}^2-A_{11}D_{11})}\frac{\partial^2 \overline{\psi}}{\partial x^2} \quad (17)$$

Substituting Eq. (15) into Eq. (17), the solution for θ is given as,

$$\theta=C_9\frac{x^2}{2}+C_{10}x+C_{11}. \quad (18)$$

Considering Eq. (16a), substituting for the derivatives of θ, $\overline{\theta}$, $\overline{\overline{\theta}}$, ψ, $\overline{\psi}$ from Eq. (15) and Eq. (18), the axial displacement variation can be obtained as,

$$u_0=-\frac{A_{13}}{A_{11}}C_5\frac{x^2}{2}-\frac{2B_{13}}{A_{11}}C_7\frac{x^2}{2}-\frac{B_{11}}{A_{11}}C_9\frac{x^2}{2}+C_{12}x+C_{13} \quad (19)$$

By substituting for the derivatives of θ, $\overline{\theta}$, $\overline{\overline{\theta}}$, ψ, $\overline{\psi}$ from Eq. (15) and Eq. (18) in Eq. (16b), the transverse displacement variation can be written as,

$$w_0=-C_9\frac{x^3}{6}+(-C_{10}-\frac{2B_{55}}{A_{55}}C_1-\frac{3D_{55}}{A_{55}}C_3)\frac{x^2}{2}+C'_{14}x+C_{14}. \quad (20)$$

where C'_{14} and C_j, j=1, $\cdots$, 14 are arbitrary constants. From equations ((18) - (20)), we see tha, slope interpolation is an order lower than the transverse displacement. This is one of the primary requirement for the element to be shear locking free. There are 15 constants in total and 14 boundary conditions, 7 on each node. Hence

there is a single dependent constant, which needs to be expressed in terms of other independent constants. Using Eq. (16c) and substituting for all the functions from Eq. (15), Eq. (18), Eq. (19) and Eq. (20), the dependent constant C'_{14} can be expressed as,

$$C'_{14} = \alpha_1 C_5 + \alpha_2 C_7 + \alpha_3 C_9 - \frac{2B_{55}}{A_{55}} C_2 - \frac{3D_{55}}{A_{55}} C_4 - C_{11}. \tag{21}$$

where,

$$\alpha_1 = \left[-\frac{B_{11}A_{13}}{A_{11}A_{55}} + \frac{B_{13}}{A_{55}} - \frac{B_{55}}{A_{55}} \right] \tag{22a}$$

$$\alpha_2 = \left[-\frac{2B_{11}B_{13}}{A_{11}A_{55}} + \frac{2D_{13}}{A_{55}} - \frac{D_{55}}{A_{55}} \right] \tag{22b}$$

$$\alpha_3 = \left[-\frac{B_{11}^2}{A_{11}A_{55}} + \frac{D_{11}}{A_{55}} \right] \tag{22c}$$

Note that the dependent constant is a function of material and sectional properties of beam. Substituting for C'_{14} in Eq. (20) the final form of the displacement field equations are given as,

$$u_0 = -\frac{A_{13}}{A_{11}} C_5 \frac{x^2}{2} - \frac{2B_{13}}{A_{11}} C_7 \frac{x^2}{2} - \frac{B_{11}}{A_{11}} C_9 \frac{x^2}{2} + C_{12}x + C_{13} \tag{23a}$$

$$w_0 = -\frac{2B_{55}}{A_{55}} C_1 \frac{x^2}{2} - \frac{2B_{55}}{A_{55}} C_2 x - \frac{2D_{55}}{A_{55}} C_3 \frac{x^2}{2} - \frac{2D_{55}}{A_{55}} C_4 x + \alpha_1 C_5 x + \alpha_2 C_7 x + (\alpha_3 x - \frac{x^3}{6}) C_9 - C_{10} \frac{x^2}{2} - C_{11} x + C_{14} \tag{23b}$$

$$\theta = C_9 \frac{x^2}{2} + C_{10}x + C_{11} \tag{23c}$$

$$\psi = C_5 x + C_6 \tag{23d}$$

$$\overline{\theta} = C_1 x + C_2 \tag{23e}$$

$$\overline{\overline{\theta}} = C_3 x + C_4 \tag{23f}$$

$$\overline{\psi} = C_7 x + C_8 \tag{23g}$$

From equation (23b), we can see that as beam becomes thin, in the penalty limit, the shear rigidity A_{55} tends to infinity, in which case, we recover the cubic polynomial interpolating functions of the Euler-Bernoulli beam. Note that we have 14 independent constants $C_j, j = 1, \cdots, 14$; which needs 7 boundary conditions, to be evaluated at the 2 nodes of the beam in the finite element system solution. It is evident that we have satisfied the static part of the governing equations.

The displacement field can be expressed as $\{u,\ w,\ \theta,\ \psi,\ \overline{\theta},\ \overline{\overline{\theta}},\ \overline{\psi}\}^T = [N_s]\{u^e\}$ where $[N_s]$ is the element shape function matrix in physical coordinate system and is of the form, $[N_s]_{(7\times14)} = \left[[N]_u\ [N]_w\ [N]_\theta\ [N]_\psi\ [N]_{\overline{\theta}}\ [N]_{\overline{\overline{\theta}}}\ [N]_{\overline{\psi}} \right]^T$. and $\{u^e\}_{(14\times1)}$ is the element nodal displacement vector.

Using these shape functions the total displacement field can be written as,

$$\left\{ \begin{array}{c} U \\ W \end{array} \right\}_{2\times1} = [\overline{N}]_{2\times14}\{u^e\}_{14\times1} \tag{24}$$

where,

$$[\overline{N}]_{2\times14} = [Z]_{2\times7}[N_s]_{7\times14} = \left[\begin{array}{c} N^U_{1\times14} \\ N^W_{1\times14} \end{array} \right] \tag{25}$$

and

$$[Z]_{2\times7} = \left[\begin{array}{ccccccc} 1 & 0 & z & 0 & z^2 & z^3 & 0 \\ 0 & 1 & 0 & z & 0 & 0 & z^2 \end{array} \right] \tag{26}$$

Next using the derived shape function, the strain displacement matrix $[B]$ is obtained, which is given by,

$$[B]_{(3\times14)} = \left[\begin{array}{c} \frac{\partial[N^U]}{\partial x} \\ \frac{\partial[N^W]}{\partial z} \\ \frac{\partial[N^U]}{\partial z} + \frac{\partial[N^W]}{\partial x} \end{array} \right] \tag{27}$$

The stiffness matrix is given by the usual expression,

$$[K]^e_{(14\times14)} = \int_0^L \int_A [B]^T [\overline{Q}][B] dA dx\,, \tag{28}$$

Next the consistent mass matrix is formulated. We formulate the matrix using the same shape functions used to derive the stiffness matrix. The

consistent mass matrix is evaluated as;

$$[M]_{(14\times14)} = \int_0^L \int_A [\overline{N}]^T \rho [\overline{N}] dA dx$$
$$= b \int_0^L \int_{\frac{-h}{2}}^{\frac{h}{2}} [N_s]^T [Z]^T \rho [Z] [N_s] dx. \quad (29)$$

the quantity, $I = b \int_{\frac{-h}{2}}^{\frac{h}{2}} [Z]^T \rho [Z]$ is the matrix containing inertia terms given by Eq. (13).

4 Numerical results and discussions

Several numerical experiments are designed to bring out the essential features of the formulated element. Although the strong reason for formulating this locking free element is to show its utility in accurately capturing the interlaminar stresses, the versatility of this element is demonstrated for static, free vibration and wave propagation problems. The main objective of this section is to show that the formulated element requires fewer degrees of freedom to capture the static, free vibration and wave propagation response as compared to many other similar elements reported in the literature, or in other words, demonstrate its super convergent property. While static and free vibration results are compared with the results published in the literature and 2D FE solutions, the wave propagation response are compared with 2D FE solutions.

4.1 Static analysis

Here a study based on deflection and stresses are made with the current element and highlighting the essential features of the current element compared to that of the other existing elements reported in the literature. In particular locking free performance of the study is demonstrated.

4.1.1 Static deflection: Shear and thickness locking studies

As mentioned in the earlier section one of the major concern in the finite element formulation based on the shear deformation theories is the shear locking and thickness locking problems, which gives deflections that are many order lower than the actual deflection.

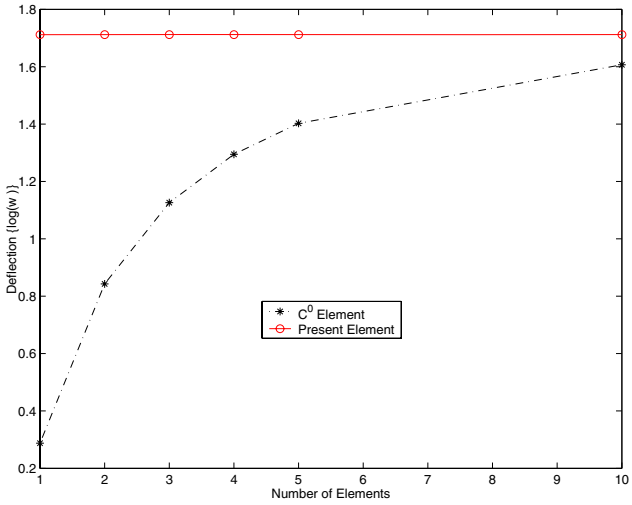

Figure 2: Convergence rate of the C^0 element compared to the present element for $\frac{L}{h} = 5$.

Here three different experiments are performed. First two cases relate to isotropic beams and the third case is for a composite beam. In the first case for L/h=5, a cantilever beam with the following non-dimensional material and sectional properties are considered. Young's modulus, E = 10.0, width, b = 1.0, ν=0.0 and the non-dimensional tip load P = 1.0.

The convergence of solution is shown in Fig. 2. The results are compared with conventional C^0 formulated element, employing full integration for the stiffness matrix. From the figure, we see that a single element of the present formulation gives a converged solution.

According to Li, Soric, Jarak, and Atluri (2005), zero Poisson's ratio does not address the thickness locking phenomena. In order to study the formulated element for thickness locking, a beam with non-zero Poisson's ratio is considered. The same material properties as given in Li, Soric, Jarak, and Atluri (2005) is considered here, which are as follows, Young's Modulus $E = 1,000,000$, length $L = 10$, $\nu = 0.25$ and a unit width $b = 1$ are used. The beam is a cantilever under tip load P. The results are compared with the theoretical solutions, as given in Li, Soric, Jarak, and Atluri (2005), which is as follows,

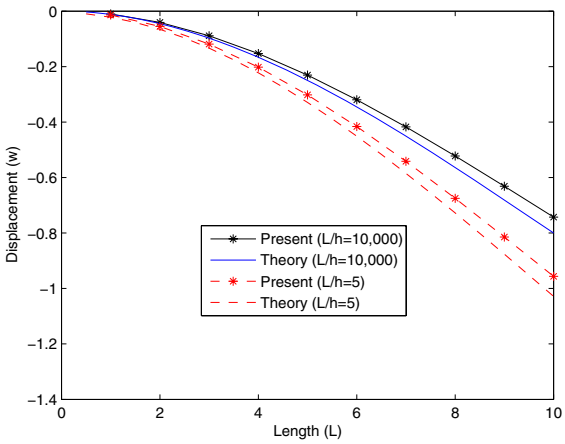

Figure 3: Comparison of the tip displacement of cantilever beam loaded at the tip.

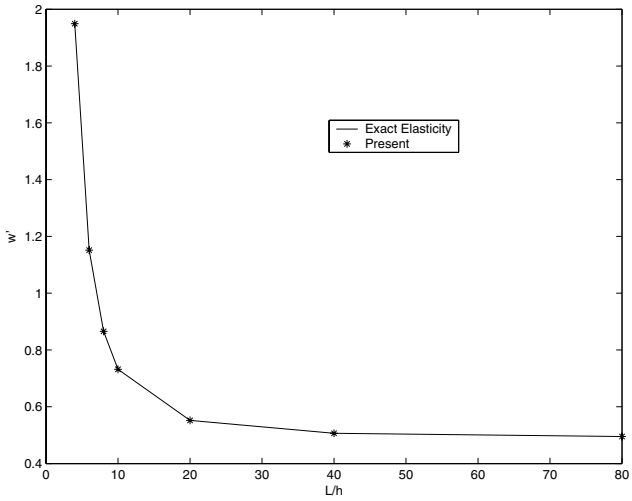

Figure 4: Non-dimensionalized deflection, w' for a beam with simply support condition under sinusoidal load.

$$w = \frac{P(1-\overline{\nu})}{6b\overline{E}I}\left[x^2(3L-x) + \frac{3\overline{\nu}}{1-\overline{\nu}}(L-x)\left(y-\frac{h}{2}\right)^2 + \frac{(4+\overline{\nu})}{(4-4\overline{\nu})}h^2x\right] \tag{30}$$

where I is the moment of inertia and given as,

$$I = \frac{bh^3}{12}$$

for plane strain case,

$$\overline{E} = E \quad \overline{\nu} = \nu$$

and for plane stress case,

$$\overline{E} = \frac{(1+2\nu)}{(1+\nu)^2}E \quad \overline{\nu} = \frac{\nu}{(1+\nu)}$$

Fig. 3 shows transverse displacement for $\frac{L}{h} = 5$ (very thick beam case) and $\frac{L}{h} = 10000$(very thin beam case). The later is an extreme case to demonstrate the locking free performance of the formulated element. been generated. The results are close to that of the theoretical solution.

The third case is for the simply supported composite beam with a sinusoidal load $p = p_0 \sin(\frac{m\pi x}{L})$, applied on the top surface with $m = 1$ and $p_0 = 1$. The material properties are as given below, $E_1 = 0.25 \times 10^8$ psi, $E_2 = E_3 = 0.1 \times 10^7$ psi, $G_{12} = G_{13} = 0.5 \times 10^6$ psi, $G_{23} = 0.2 \times 10^6$ psi, $\nu_{12} = \nu_{13} = \nu_{23} = 0.25$. The results of normalized deflection $w' = \frac{100E_2h^2w(l/2,0)}{p_0L^4}$ for different $\frac{L}{h}$ ratios are generated and are compared with the exact elasticity solutions given by, Pagano (1969). A very good agreement with the exact solutions can be observed from Fig. 4.

4.1.2 Interlaminar stresses

The results of the interlaminar stresses obtained from the formulated element is compared with those availabe in literature. A comparison is made with Vinayak, Prathap, and Naganarayana (1996a), where the authors used higher order finite elements (BM3 and BM4), which is based on the same beam theory as considered here. BM3 is a 3 noded beam element and BM4 is a 4 noded beam element. The same material properties and the geometric properties as used in this paper, is used here to perform the present numerical experiments. *For Isotropic beam*:
The geometry of the beam is given by length L = 10.0, thickness h = 1.0 and width b = 1.0. The Young's modulus is assumed as E = 1000.0, Poisson's ratio ν = 0.0 and a uniformly distributed

Table 3: Comparison of Transverse shear stress τ_{xz} for beam under uniformly distributed load at x =5.5

z/h	$\frac{L}{h}$=10		$\frac{L}{h}=1$	
	Present	Vinayak(1996)	Present	Vinayak(1996)
-0.5	0.0	0.0	0.0	0.0
-0.4	2.4312	2.4299	0.2611	0.2547
-0.3	4.3203	4.3199	0.4517	0.4503
-0.2	5.6696	5.6700	0.5859	0.5861
-0.1	6.4792	6.4800	0.6637	0.6623
0.0	6.7490	6.7500	0.6851	0.6800
0.1	6.4792	6.4800	0.6500	0.6414
0.2	5.6693	5.6700	0.5585	0.5496
0.3	4.3199	4.3199	0.4106	0.4084
0.4	2.4306	2.4299	0.2064	0.2232
0.5	0.0	0.0	0.0	0.0

Table 1: Comparison of axial stress σ_{xx} in a isotropic cantilever beam with uniformly distributed load on the top surface for L/h=10 at x = 5.5.

z/h	Vinayak(1996) BM4	Vinayak(1996) BM3	Present
0.5	60.550	60.800	60.901
0.4	48.584	48.784	48.792
0.3	36.522	36.672	36.636
0.2	24.388	24.488	24.444
0.1	12.206	12.256	12.228
0.0	0.0	0.0	0.0

Table 2: Comparison of Transverse normal stress σ_{zz} under uniformly distributed load on top surface and on mid-plane for L/h=10 at x = 5.5.

z/h	Vinayak(1996)	Present	$\sigma_{zz}(ls)$
-0.5	-0.097	-0.0967	-0.1
-0.4		0.0226	
-0.3		0.1419	
-0.2		0.2613	
-0.1		0.3806	
0.0	0.492	0.4999	0.5
0.1		0.6192	
0.2		0.7386	
0.3		0.8579	
0.4		0.9772	
0.5	1.081	1.0965	1.1

load (*udl*), p = 1.0 is used to load the beam on the top surface. A mesh of 10 elements is used for both in the present case and in the above paper. The test is done on a cantilever beam, that is fixed at one end and free at the other end. The results are shown in Table 1.

The results shows good agreement with both BM3 and BM4 model of Vinayak, Prathap, and Naganarayana (1996a) BM3 and BM4 elements. The results of transverse normal stress for the same model is presented in Table 2 and even here the close agreement between the two elements can be noticed. As given in Pratap (1993), it is known that finite element displacement method solutions seek strains/stresses in a least square sense and hence the values predicted in the least squares sense $\sigma_{zz}(ls)$ has been given in the table for comparison. Similarly Table 3 shows a comparison of the transverse shear stress for the present element for two different $\frac{L}{h}$ namel $\frac{L}{h}$ =10 and $\frac{L}{h}$=1 respec-

tively.

It can be seen that the results are in good agreement. It can be noted that the results for $\frac{L}{h} = 10$ case of Vinayak, Prathap, and Naganarayana (1996a) is symmetric about the mid-plane. This is because the load would have been placed on the mid-plane of the beam and is to be treated as an imaginary case. The cantilever beam model has 70 degree of freedom(dof) with the present element formulation as opposed to 140 dof for BM3 and 210 dof for BM4 respectively. Tables 1, 2, 3 demonstrate the fast convergence property of the element, which saves the computational time.

For Composite beam:

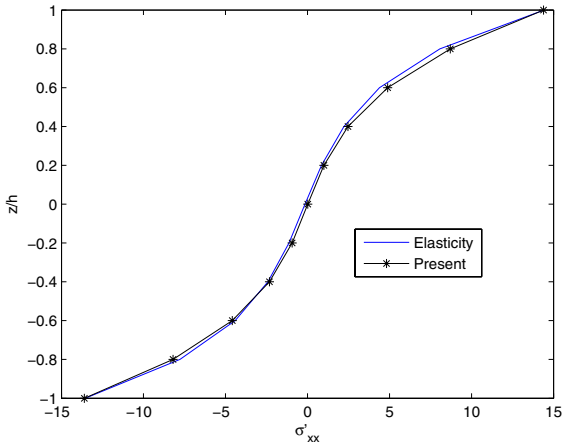

Figure 5: Variation of bending stress for a sinusoidal load on a beam with $\frac{L}{h} = 4$.

A orthotropic graphite/epoxy material beam with the following material properties as given in Pagano (1969) is considered here, $E_1 = 0.25 \times 10^8$ psi, $E_2 = E_3 = 0.1 \times 10^7$ psi, $G_{12} = G_{13} = 0.5 \times 10^6$ psi, $G_{23} = 0.2 \times 10^6$ psi, $\nu_{12} = \nu_{13} = \nu_{23} = 0.25$. The boundary condition is simply supported and a sinusoidal load, p = $p_0 \sin(\frac{m\pi x}{L})$ is applied on the top surface with $m = 1$ and $p_0 = 1$. First the case of a unidirectional composite beam with 0^0 ply and $\frac{L}{h} = 4$ is considered. The results of interlaminar stresses and normal stresses are shown in Fig. 5, Fig. 6 and Fig. 7 along with those of the exact elasticity solution of Pagano, Pagano (1969).

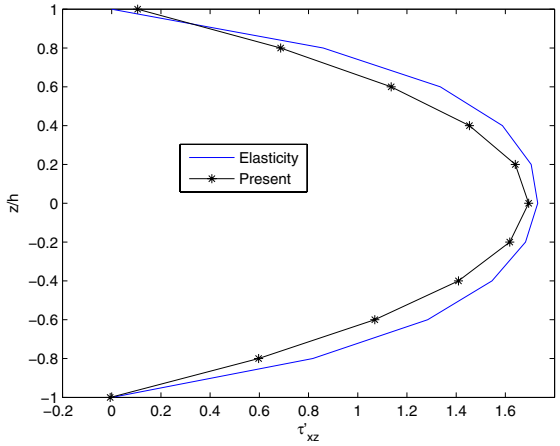

Figure 6: Variation of transverse shear stress for a sinusoidal load on a beam with $\frac{L}{h} = 4$.

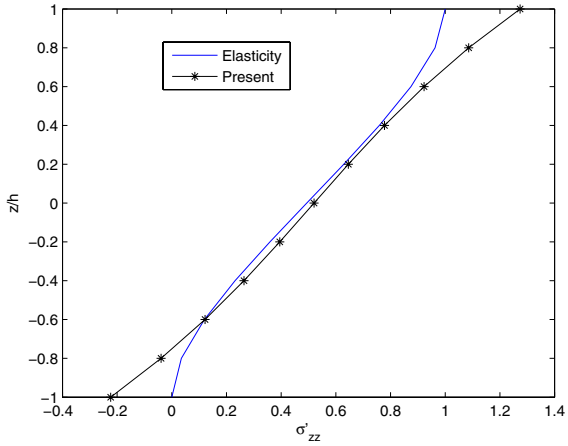

Figure 7: Variation of transverse normal stress for a sinusoidal load on a beam with $\frac{L}{h} = 4$.

The figures show that the results of the present element are very close to the elasticity solutions. The normalized values are given as,

$$\sigma'_{xx} = \frac{\sigma_{xx}(L/2,z)}{p_0} \quad \sigma'_{zz} = \frac{\sigma_{zz}(L/2,z)}{p_0}.$$
$$\tau'_{xz} = \frac{\tau_{xz}(0,z)}{p_0}. \tag{31}$$

Next, a symmetric ply stacking of $[0^\circ/90^\circ/0^\circ]$ composed of 3 layers and all plies are of equal

thickness with $\frac{L}{h} = 10.0$ is considered. The result of non-dimensional axial stress σ'_{xx} is compared in Table 4 with that of the exact solutions of Pagano (1969) and of Vinayak, Prathap, and Naganarayana (1996a). The nondimensional quantity is given as in Eq. 31. From Table 4 it can be seen that the performance of the present element is very good.

Table 4: Comparison of non-dimensional normal stress σ'_{xx} in a composite beam $[0^\circ/90^\circ/0^\circ]$ with sinusoidal load on the top surface, with simply supported boundary condition for L/h=10

z/h	Elasticity	Present	Vinayak(1996)
-0.5	-72.820	-72.160	-71.958
-0.4	-52.923	-50.777	-50.678
-0.3	-32.830	-34.033	-34.013
-0.2	-16.103	-20.766	-20.806
-1/6	-11.282	-16.580	-16.972
1/6	11.590	16.929	16.734
0.2	16.410	20.795	20.584
0.3	32.830	34.124	33.856
0.4	51.282	50.954	50.611
0.5	72.820	72.449	72.006

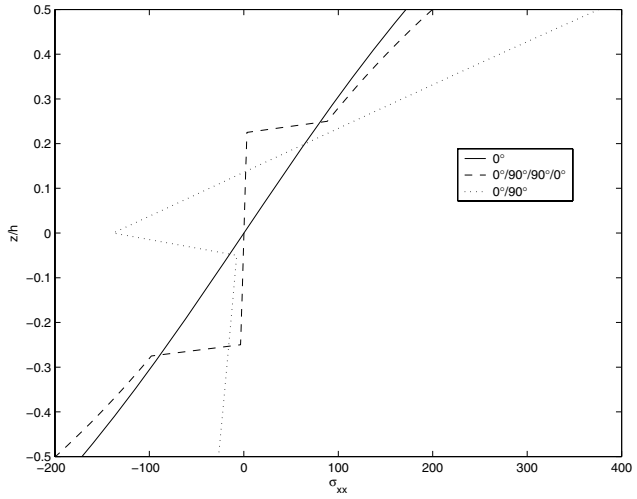

Figure 8: Variation of bending stress, $\sigma_{xx}(\frac{L}{2}, z)$, for a beam with simply support condition under uniformly distributed load for different ply configuration.

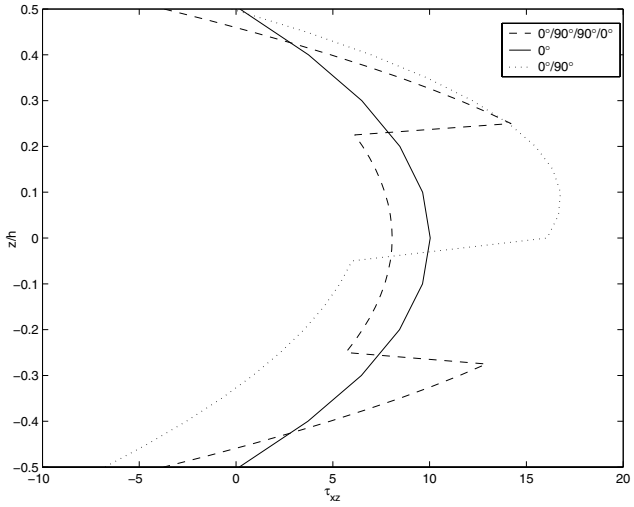

Figure 9: Variation of Transverse stress, $\tau_{xz}(0, z)$, for a beam with simply support condition under uniformly distributed load for different ply configuration.

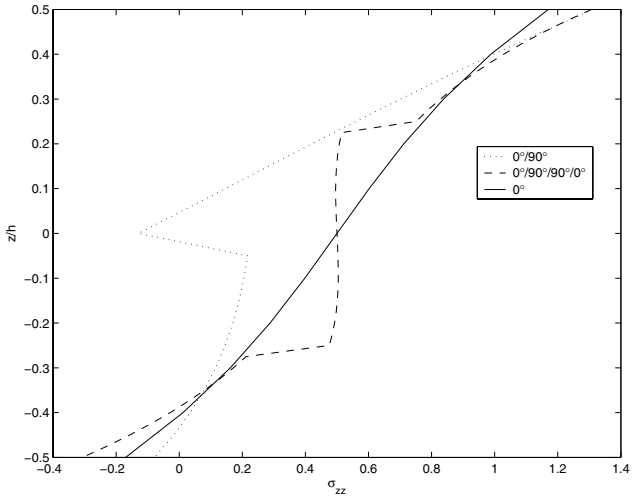

Figure 10: Variation of transverse normal stress, $\sigma_{zz}(\frac{L}{2}, z)$, for a beam with simply support condition under uniformly distributed load for different ply configuration.

Similarly an uniformly distributed load(*udl*) of 1.0 is applied to a composite beam of $\frac{L}{h} = 15$,

which is simply supported with different ply configurations [0°/90°/90°/0°], [0°/90°] and [0°] . The stresses are measured at $\sigma_{xx}(\frac{L}{2},z)$, $\tau_{xz}(0,z)$ and $\sigma_{zz}(\frac{L}{2},z)$ and are shown in Fig. 8, Fig. 9 and Fig. 10. The parabolic nature of transverse shear stress, the cubic nature of normal stresses and the stress jumps for the asymmetric composite can be observed.

4.2 Free vibration analysis

Here different numerical experiments are performed to compare the performance of the present element with the element based on HSDT of Heyliger and Reddy (1988), HSDT of Kant, Marur, and Rao (1998) and HSDT of Marur and Kant (1996) respectively. The total displacement field of HSDT of Heyliger and Reddy (1988) is given as,

$$U(x,y,z,t) = u_0(x,t) + z\theta(x,t) + c_0 z^3\left(\theta(x,t) + \frac{\partial w(x,t)}{\partial x}\right), \tag{32a}$$

$$W(x,y,z,t) = w_0(x,t)\,, \tag{32b}$$

The displacement field of HSDT of Kant, Marur, and Rao (1998) is given as,

$$U(x,y,z,t) = u_0(x,t) + z\theta(x,t) + z^2\overline{\theta}(x,t) + z^3\overline{\overline{\theta}}(x,t)\,, \tag{33a}$$

$$W(x,y,z,t) = w_0(x,t) + z\psi(x,t) + z^2\overline{\psi}(x,t) + z^3\overline{\overline{\psi}}(x,t)\,, \tag{33b}$$

and of HSDT of Marur and Kant (1996) is given as,

$$U(x,y,z,t) = u_0(x,t) + z\theta(x,t) + z^2\overline{\theta}(x,t) + z^3\overline{\overline{\theta}}(x,t)\,, \tag{34a}$$

$$W(x,y,z,t) = w_0(x,t)\,, \tag{34b}$$

To study the behavior of the present finite element model for free vibration, we first consider a symmetric cross-ply [0°/90°/0°] beam and a asymmetric beam [0°/90°] with the following material properties; $E_1/E_2 = 40$, $G_{12} = G_{13} = 0.6E_2$, $G_{23} = 0.5E_2$, $\nu_{12} = 0.25$.

The non-dimensional natural frequency is used as comparative quantity and is given by,

$$\overline{\omega}_2 = \omega L^2\sqrt{\frac{\rho}{E_2 h^2}}\,, \tag{35}$$

where ω is the natural frequency. The results are presented in Table 5 for [0°/90°/0°] ply stacking and Table 6 for [0°/90°] ply stacking and are compared for various $\frac{L}{h}$ and various boundary conditions (C-C clamped-clamped, H-H Hinge-Hinge, C-H Clamped-Hinge,& C-F clamped-Free). A mesh of 10 elements of current formulation is used. Heyliger and Reddy (1988) has generated results using state space concept. The non-dimensional natural frequencies of the present element is compared with the results reported in Heyliger and Reddy (1988), and with the MSC Nastran CQUAD4 2D finite elements (FE). The total degrees of freedom involved in the 2D FE formulation is around 2000.

Table 5: Comparison of non-Dimensional fundamental frequency $\overline{\omega}_2$ of a symmetric cross-ply [0°/90°/0°] beams for various boundary conditions.

L/h		H-H	C-H	C-C	C-F
5	2D FE	8.985	9.666	10.598	4.053
	Present	8.993	9.687	10.681	4.061
	% Error	0.089	0.217	0.783	0.197
	Reddy	9.208	10.239	11.603	4.232
	% Error	2.482	5.928	9.483	4.416
10	2D FE	13.218	16.028	18.884	5.278
	Present	13.224	16.088	18.994	5.282
	% Error	0.045	0.374	0.583	0.0758
	Reddy	13.614	16.599	19.712	5.495
	% Error	2.996	3.563	4.385	4.111

The Tables 5, 6 shows the percentage error of the responses predicted by the current element and the element of Heyliger and Reddy (1988) to that of the 2D finite element result. From these tables we can see that the HSDT of Heyliger and

Table 6: Comparison of non-Dimensional fundamental frequency $\overline{\omega}_2$ of asymmetric cross-ply $[0^\circ/90^\circ]$ beams for various boundary conditions.

L/h		H-H	C-H	C-C	C-F
5	2D FE	5.655	7.029	8.472	2.273
	Present	5.717	7.266	8.814	2.316
	% Error	1.096	3.371	4.037	1.892
	Reddy	6.128	8.033	10.026	2.386
	% Error	8.364	14.284	18.343	4.971
10	2D FE	6.765	9.550	12.510	2.510
	Present	6.802	9.761	12.911	2.525
	% Error	0.547	2.209	3.205	0.598
	Reddy	6.945	10.129	13.660	2.544
	% Error	2.661	6.063	9.193	1.355

Table 7: Comparison of non-dimensional natural frequencies $\overline{\omega}_1$ of a composite beam of $[0^\circ/0^\circ/90^\circ/90^\circ/90^\circ/90^\circ/0^\circ/0^\circ]$ ply stacking with simply supported boundary condition for L/h=15

mode	Kant(1998)	Present	2D FE
1	2.516	2.4818	2.4817
2	8.669	8.322	8.272
3	16.320	15.495	15.148
4	24.371	23.310	22.189

Reddy (1988) is not able to capture the fundamental mode accurately. The performance of the present element compared to this HSDT is very good. This can be attributed to the the inclusion of the lateral contraction in the model, which helps to simulate the 2-D state of stress better using 1-D beam model. It can be observed from the tables that the clamped boundary condition cases give more error. The reason for this is that the stress is singular and acts like a re-entrant corner. This has an impact on natural frequency; as it also depends on the stiffness of the system. This aspect is clearly explained by RamaMohan, Naganarayana, and Prathap (1994).

Table 8: Comparison of non-dimensional natural frequencies $\overline{\omega}_1$ of a composite beam of $[0^\circ/0^\circ/90^\circ/90^\circ/90^\circ/90^\circ/0^\circ/0^\circ]$ ply stacking with simply supported boundary condition for L/h=5

mode	Kant(1998)	Present	2D FE
1	1.820	1.6886	1.6834
2	4.528	4.1222	4.0078
3	7.201	6.3244	6.2576
4	9.814	9.4028	8.4668

Free vibration results for different modes are compared with another HSDT proposed by Kant, Marur, and Rao (1998). They have presented analytical solutions for computing the natural frequencies. The results are also compared with 2D FE solutions. The results are generated for different ply stacking sequence. The non-dimensional fundamental frequency in this case for comparison is given as,

$$\overline{\omega}_1 = \omega L^2 \sqrt{\frac{\rho}{E_1 h^2}}\,, \tag{36}$$

For the first case; the data is taken from Kant, Marur, and Rao (1998) and are the following.
Material AS4/3501-6/ Graphite-Epoxy, Lamination scheme $[0^\circ/0^\circ/90^\circ/90^\circ/90^\circ/90^\circ/0^\circ/0^\circ]$; b = 1 m, E_1 = 144.8 GPa, E_2 = 9.65 GPa, G_{12} = 4.14 GPa, ρ = 1389.23 kg/m^3. ν_{12}=0.3. Two cases are considered L=15, h = 1 and L=15, h=3, both with simply supported boundary condition. 5 beam elements of the present formulation are used to get the results which are shown in Table 7($\frac{L}{h}$=15) and Table 8($\frac{L}{h}$=5) respectively for the first four modes. The results show that the present element is able to accurately capture the natural frequencies predicted by the theoretical solutions.

Results are generated for the second case with a different lamination scheme given by $[0^\circ/0^\circ/90^\circ/90^\circ/0^\circ/0^\circ]$ for symmetric case and $[0^\circ/90^\circ/0^\circ/90^\circ/0^\circ/90^\circ]$ for asymmetric case and the results are presented in Table 9 for the first

Table 9: Comparison of non-dimensional natural frequencies $\overline{\omega}_1$ of a thick beam (L/h=5) with simply supported boundary condition.

mode	Kant(1998)	Present	2D FE	Kant(1996)	Present	2D FE
	$[0°/0°/90°/90°/0°/0°]$			$[0°/90°/0°/90°/0°/90°]$		
1	1.657	1.5903	1.5768	1.416	1.3569	1.3564
2	3.910	3.7578	3.6086	3.531	3.3827	3.2952
3	6.138	6.0284	5.5689	5.675	5.4876	5.1953
4	8.323	7.8494	7.4925	7.795	7.6063	7.0444

four modes. For the asymmetric case the results are compared with the HSDT Marur and Kant (1996) where they have formulated the element based on the displacement field as given in the above Eq.(34). The element has 5 dof per node. The data for this example are given as, L = 762 mm h = 152.4 mm, b = 25.4 mm, $E_1 = 0.525 \times 10^6 N/mm^2$, $E_2 = 0.21 \times 10^5 N/mm^2$, $G_{12} = 0.105 \times 10^5 N/mm^2$, $\rho = 800 kg/m^3$.

As in the previous case 5 beam elements of the present formulation is used. The results presented in Table.9 show good comparison for $\frac{L}{h}$=5.

4.3 Wave Propagation Analysis

A wave propagation problem is a multi-modal phenomenon; where phase information is very important. The frequency content of the forcing function is very high in the wave propagation problems. At higher frequencies, the wavelength is small, and this requires the element size to be comparable to wavelength, so as to capture all the higher modes accurately. This makes the Finite Element system size very large.

The aim of the present section is to study the efficieny of the element to capture not only the wave propagation response with smaller system size but also the inter-laminar dynamic stresses. A cantilever beam with a tip impact load is considered. The impact load is a transverse pulse with a peak amplitude of 4.4 Newtons and 50 μs duration as shown in the inset of Fig. 11. The Fourier transform (FFT) of the load shows a very high frequency (44 KHz) content as shown in Fig. 11. Time marching scheme using Newmark α- β integration method, is employed to obatin the the solutions of the equilibrium equations.

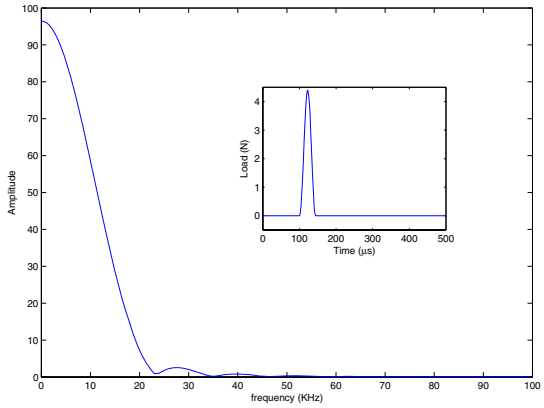

Figure 11: Fourier Transform of Impact Pulse load (inset) using FFT.

The geometric and material properties of the beam considered is taken as, L = 100 m, b = 1 m, h = 1 m, Material is AS4/3501-6 graphite epoxy, E_1 = 144.8 GPa, E_2 = 9.65 GPa, $G_{12} = G_{13}$ = 4.14 GPa, G_{23} = 3.45 GPa, ρ = 1389.23 kg/m^3. ν_{12}=0.3.

4.3.1 Dynamic response

First the axial response is obtained where the beam is excited by an impact load applied axially, at the tip of the cantilever beam. Fig. 12 shows a plot of the axial velocity with time. The results are comapred with another HSDT theory of Murthy, Mahapatra, Badarinarayana, and Gopalakrishnan

(2005). In both the beam models the beam is modeled with 100 elements. The plot shows no much deviation between both the theories for the axial response case. This can be expected since the axial displacement field, which is same for both the theories.

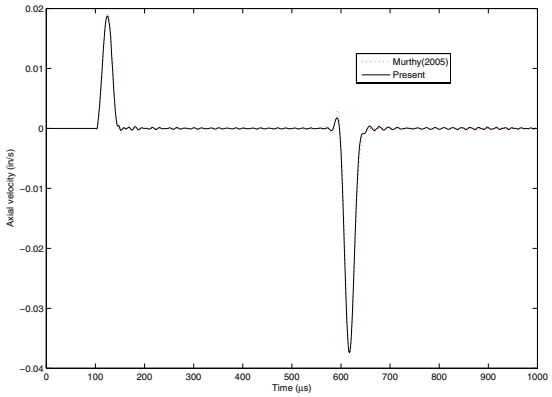

Figure 12: Comparison of Axial velocity response for $\frac{L}{h} = 100$.

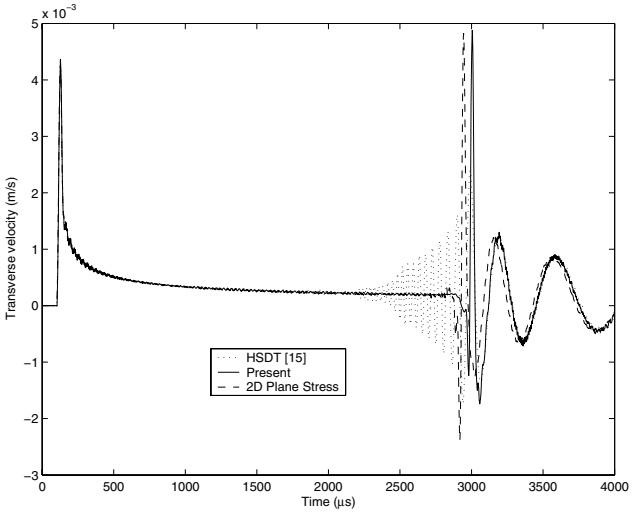

Figure 13: Comparison of Transverse velocity response for $\frac{L}{h} = 100$.

Next, we obtain the transverse response where the impact load is applied in the transverse direction at the tip of the cantilever beam. The beam is modelled with 1000 elements of Murthy, Mahapatra, Badarinarayana, and Gopalakrishnan (2005) and of the present theory. A very fine mesh of MSC Nastran CQUAD4 element with 2D plane stress property is used to compare the results. The total degrees of freedom (dof) in each of the cases are as follows; 4000 dof for Murthy, Mahapatra, Badarinarayana, and Gopalakrishnan (2005) case, 7000 dof for the present case and 12500 dof for the 2D FE case. Fig. 13 shows the plot of all the three cases. The results show that present element and 2D FE show excellent agreement. Murthy, Mahapatra, Badarinarayana, and Gopalakrishnan (2005) element show a small period error in the occurrences of reflection.

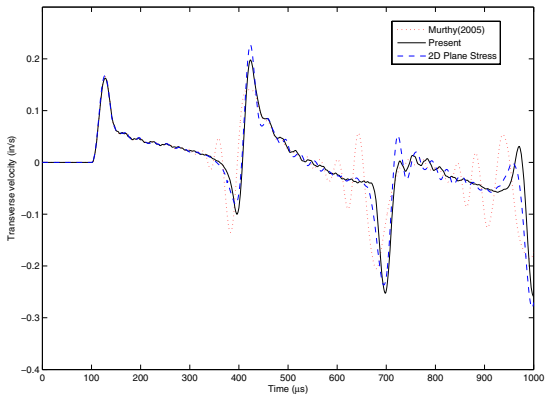

Figure 14: Comparison of Transverse velocity response for $\frac{L}{h} = 10$.

A similar plot with $\frac{L}{h}$=10 for the transverse velocity is shown in Fig. 14. In this case, smaller $\frac{L}{h}$ results in shear deformation participating significantly in the response. This results in decrease in the wave velocity and hence early arrival of reflections as compared to Fig. 13, whose results are more close to EBT theory. The figure also shows that the results predicted by Murthy, Mahapatra, Badarinarayana, and Gopalakrishnan (2005) is completely out of phase and the present element predicts results very close to the 2D FE solution.

4.3.2 Dynamic inter-laminar stresses

The inter-laminar stresses developed due to impact load is much higher than those with the static load. Here the same beam example as mentioned in the previous section with L/h=100 with a impluse load at the free end, applied transversely in the Z direction, is considered for generating the stress history. The beam is made up of 4 layers of the same AS/3501-6 graphite-epoxy material and assumed to be tightly glued to each other. The axial/bending stress history, transverse shear stress history and the transverse normal stress hsitory at different ($\frac{z}{h}$) locations through the thickness are shown in Fig. 15, Fig. 16 and Fig. 17 respectively.

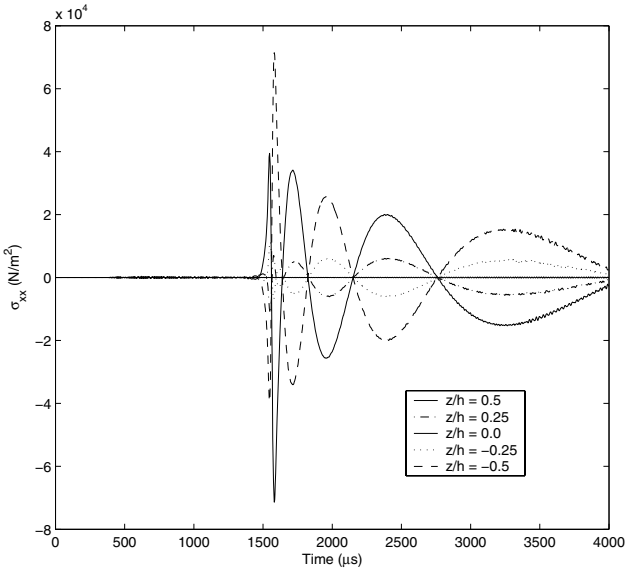

Figure 15: Axial stress history at the fixed end of the cantilever for $\frac{L}{h} = 100$.

From the plots, we can observe that, the peak stresses occur at 1500 μs. This is the time taken by the incident pulse to hit the fixed boundary and generate a reflection. As expected, the transverse normal stress is negligible. The plot for transverse shear stress is at the tip of the cantilever beam and hence peak stresses through the thickness is shown at 100 μs.

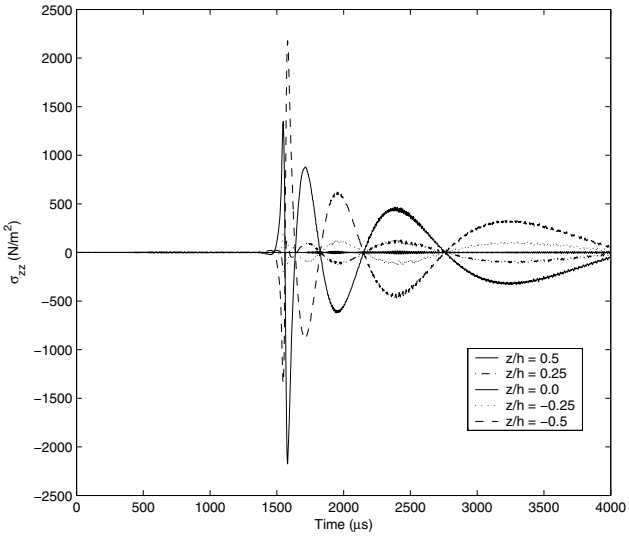

Figure 16: Transverse normal stress history at the fixed end of the cantilever for $\frac{L}{h} = 100$.

5 Conclusions

This paper presents a locking free finite element formulation for laminated composite beams using higher order shear deformation theory with the inclusion of the lateral contraction effect. The element formulated is shown to have superconvergent property. This is due to the use of interpolation functions for the axial, transverse and shear degrees of freedom, which satisfies the corresponding governing differential equations exactly. Due to enforcement of equilibrium, many coefficients in the interpolation function are material and section property dependent and hence in the penalty limit of beam becoming thin, those constants that were responsible for shear locking automatically vanish giving a superior performance. Hence, the present formulation does not require special treatments like, field consistency and reduced integration.

The study has brought forth the cubic accuracy expected with that of the normal stresses σ_{xx}, σ_{zz} and parabolic for the transverse shear stresses τ_{xz}. The transverse stresses reported here, are in good agreement with exact elasticity solutions of Pagano (1969) and other works reported in the available literature.

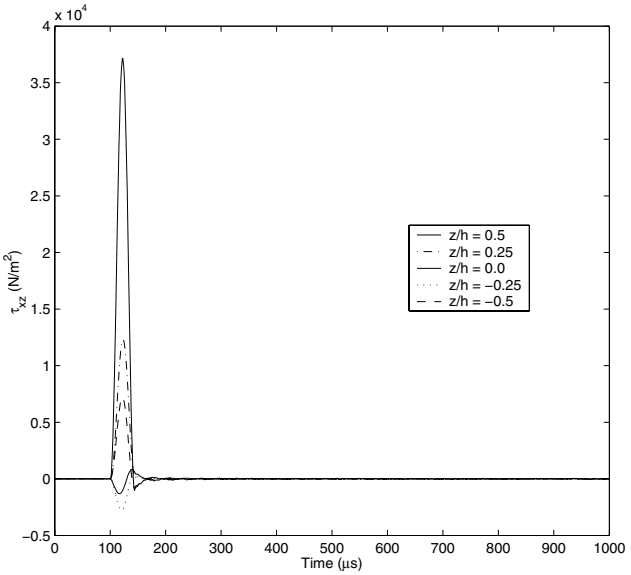

Figure 17: Transverse shear stress history at the tip of the cantilever for $\frac{L}{h} = 100$.

In addition to its great utility in predicting inter-laminar stresses, the formulated element will find its usefulness in solving wave propagation problems, where the frequency content of input signal is usually very high (of the order of kHz or higher). Solution of wave propagation problems through finite elements requires very fine mesh to capture higher order modes accurately. Since the formulated element satisfies the static part of the governing equation, the stiffness is accurately represented, although the inertial distribution is approximate. According to Strang and Fix (1973), the error introduced due to approximate stiffness distribution is an order higher than the error due to approximate mass distribution. This is shown in the numerical studies of free vibration and the wave propagation problems, which brought out the excellent convergent property of the element when compared with the 2D FEM solutions.

In addition to mechanical loading, thermal loading can result in inter-laminar stresses of significant amounts. This is particularly important in composite beams with unsymmetrical lay up. The thermal loading can introduce unsymmetrical bending due to stiffness coupling, which can introduce additional inter-laminar stresses. This will be considered in the future research work.

Acknowledgement: Authors acknowledge the help given by Dr. D. Roy Mahapatra, currently the Post-doctoral research at Wilfred Lauier University, Cannada, towards deriving the governing equations and their solutions.

References

Atluri, S. N. (2005): *Methods of Computer Modeling in Engineering and the Sciences*. Tech Science Press.

Cazzani, A.; Garusi, E.; Tralli, A.; Atluri, S. N. (2005): A four-node hybrid assumed-strain finite element for laminated composite plates. *CMC: Computers, Materials and Continua*, vol. 2, no. 1, pp. 23–38.

Chakraborty, A.; Gopalakrishnan, S. (2003): Poisson's effects in deep laminated beams. *Mechanics of Advanced materials and Structures*, vol. 10, no. 3, pp. 205–225.

Doyle, J. F. (1997): *Wave Propagation in Structures*. Springer-Verlag.

Gopalakrishnan, S. (2000): A deep rod finite element for structural dynamics and wave propagation problems. *International Journal for numerical methods in Engineering*, vol. 48, pp. 731–744.

Heyliger, P. R.; Reddy, J. N. (1988): A higher order beam finite element for bending and vibration problems. *Journal of Sound and Vibration*, vol. 126, pp. 309–326.

JihanKim; YongHyupKim; Lee, S. W. (2004): Asymptotic Postbuckling Analysis of Composite and Sandwich Structures via the Assumed Strain Solid Shell Element Formulation. *CMES: Computer Modeling in Engineering and Sciences*, vol. 6, no. 3, pp. 263–276.

Kant, T.; Marur, S. R.; Rao, G. S. (1998): Analytical solution to the dynamic analysis of laminated beams using higher order theory. *Composite Structures*, vol. 40, pp. 1–9.

Kim, T.; Atluri, S. N. (1994): Interlaminar stresses in compoiste laminates under out-of-plane shear/bending. *AIAA Journal*, vol. 32, no. 8, pp. 1700–1708.

Kouri, J. V.; Atluri, S. N. (1993): Analytical modelling of laminated composites. *Composites Science and Technology*, vol. 46, pp. 335–344.

Li, Q.; Soric, J.; Jarak, T.; Atluri, S. N. (2005): A Locking Free meshless local Petrov-Galerkin formulation for thick and thin plates. *Journal of Computational Physics*, vol. 208, pp. 116–133.

Lo, K. H.; Christensen, R. M.; Wu, E. M. (1977): A higher order theory of plate deformation. Part1: Homogeneous Plates. *Journal of Applied Mechanics*, pp. 663–668.

Lo, K. H.; Christensen, R. M.; Wu, E. M. (1977): A higher order theory of plate deformation. Part1: Laminated Plates. *Journal of Applied Mechanics*, pp. 669–676.

Mahapatra, D. R.; Gopalakrishnan, S. (2003): A spectral finite element model for analysis of axial-flexural-shear coupled wave propagation in laminated composite beams. *Composite Structures*, vol. 59, pp. 67–88.

Marur, S. R.; Kant, T. (1996): Free vibration analysis of fiber reinforced composite beams using higher order theories and finite element modelling. *Journal of Sound and Vibration*, vol. 194, no. 3, pp. 337–351.

Murthy, M. V. V. S.; Mahapatra, D. R.; Badarinarayana, K.; Gopalakrishnan, S. (2005): A refined higher order finite element for asymmetric composite beams. *Composite Structures*, vol. 67, pp. 27–35.

Pagano, N. J. (1969): Exact solution for composite laminates in cylindrical bending. *Journal of Composite Materials*, vol. 3, pp. 398–410.

Pratap, G. (1993): *The Finite Element Method in Structural Mechanics*. Kluwer Academic Publishers.

RamaMohan, P.; Naganarayana, B. P.; Prathap, G. (1994): Consistent and variationally correct finite elements for higher-order laminated plate theory. *Composite Structures*, vol. 29, pp. 445–456.

Reddy, J. N. (1997): *Mechanics of Laminated Composite Plates, Theory and Analysis*. CRC Press.

Strang, G.; Fix, G. J. (1973): *An analysis of finite element method*. Englewoodcliffs, Prentice-Hall.

Vinayak, R. U.; Prathap, G.; Naganarayana, B. P. (1996): Beam elements based on a Higher order theory - Part1: Formulation and analysis of performance. *Computers and Structures*, vol. 58, no. 4, pp. 775–789.

Vinayak, R. U.; Prathap, G.; Naganarayana, B. P. (1996): Beam elements based on a Higher order theory - Part2: Boundary layer sensitivity and stress oscillations. *Computers and Structures*, vol. 58, no. 4, pp. 791–796.

Whitney, J. H. (1973): Shear correction factors for orthotropic laminates under static load. *Journal of Applied Mechanics*, pp. 302–304.